Atrophy of calf muscles by unloading results in an increase of tissue sodium concentration and fat fraction decrease: a ^{23}Na MRI physiology study

D. A. Gerlach, K. Schopen, P. Linz, B. Johannes, J. Titze, J. Zange & J. Rittweger

European Journal of Applied Physiology

ISSN 1439-6319

Eur J Appl Physiol
DOI 10.1007/s00421-017-3647-4

Springer

Eur J Appl Physiol
DOI 10.1007/s00421-017-3647-4

ORIGINAL ARTICLE

Atrophy of calf muscles by unloading results in an increase of tissue sodium concentration and fat fraction decrease: a ^{23}Na MRI physiology study

D. A. Gerlach[1] · K. Schopen[1,2] · P. Linz[3,4] · B. Johannes[1] · J. Titze[4,5] · J. Zange[1] · J. Rittweger[1,6]

Received: 3 March 2017 / Accepted: 17 May 2017

Abstract
Purpose ^{23}Na MRI demonstrated increased tissue sodium concentrations in a number of pathologies. Acute atrophy results in muscle fibre volume shrinking that may result in a relative increase of extracellular volume and might affect sodium concentration. Thus, we hypothesized that local unloading of the calf muscles would lead to a decrease in muscle volume and an increase in muscle tissue sodium concentration.
Method One lower leg of 12 healthy male subjects was submitted to a 60 day long period of unloading using the Hephaistos orthosis, while the other leg served as control. ^{23}Na MRI and 2D PD-weighted Dixon turbo spin echo were obtained from the control and orthosis leg using a 3T scanner. For quantification, a sodium reference phantom was used with 10, 20, 30, and 40 mmol/L NaCl solution.
Result Tissue sodium concentration (TSC) increased as an effect of unloading in the orthosis leg. Relative increases were 17.4 ± 16.8% ($P = 0.005$) in gastrocnemius medialis muscle, 11.1 ± 12.5 ($P = 0.037$) in gastrocnemius lateralis muscle, 16.2 ± 4.7% ($P < 0.001$) in soleus muscle, 10.0 ± 10.5% ($P = 0.009$) in the ventral muscle group, and 10.7 ± 10.0% ($P = 0.003$) in the central muscle group, respectively. TSC in the control leg did not significantly change. In the orthosis leg, muscle volume decreased as follows: medial gastrocnemius muscle: −5.4 ± 8.3% ($P = 0.043$) and soleus muscle: −7.8 ± 15.0% ($P = 0.043$).
Conclusion Unloading atrophy is associated with an increase in muscle sodium concentration. ^{23}Na MRI is capable of detecting these rather small changes.

Keywords Sodium · MRI · ^{23}Na MRI · Tissue sodium concentration (TSC) · Quantification · Muscle unloading

Abbreviations

FoV	Field of view (FoV)
LME	Linear mixed effects
PD	Proton density
ROI	Regions of interest
SNR	Signal-to-noise ratio
TSC	Tissue sodium concentration
TSE	Turbo spin echo
TA	Acquisition time
TE	Echo time
TR	Repetition time
T_2	Transversal relaxation time

Communicated by Guido Ferretti.

✉ D. A. Gerlach
darius.gerlach@dlr.de

[1] Division of Space Physiology, Institute of Aerospace Medicine, German Aerospace Center (DLR), Cologne, Germany

[2] Department of Molecular and Cellular Sport Medicine, German Sport University Cologne, Cologne, Germany

[3] Department of Radiology, University Hospital Erlangen, Erlangen, Germany

[4] Interdisciplinary Center for Clinical Research, Nikolaus-Fiebiger-Center for Molecular Medicine, Friedrich-Alexander-University Erlangen-Nürnberg, Erlangen, Germany

[5] Division of Clinical Pharmacology, Vanderbilt University Medical Center, Nashville, TN, USA

[6] Department of Paediatrics and Adolescent Medicine, University of Cologne, Cologne, Germany

Published online: 22 May 2017

Introduction

The physiological interest in the independency of water and sodium balance (Drummer et al. 2000) and in the non-osmotical storage of sodium in skin and muscle tissue (Titze et al. 2003) is currently sharply increasing. As a consequence, ^{23}Na MRI has recently also become a prominent topic in MRI methodology and pathophysiology as well. Some groups have focused on method development and feasibility studies and discussed their potential for diagnostics (Lu et al. 2010; Nagel et al. 2009). Clinically relevant topics have been addressed, such as hypertension (Kopp et al. 2012, 2013), kidney failure (Dahlmann et al. 2015), cancer diagnostics (Ouwerkerk et al. 2003), muscle diseases (Constantinides et al. 2000; Nagel et al. 2011; Weber et al. 2012), cartilage degeneration (Borthakur et al. 2000, 2006), spinal disc morphology (Ooms et al. 2008), and multiple sclerosis (Inglese et al. 2010; Maarouf et al. 2014; Paling et al. 2013).

Sodium has a nuclear spin of 3/2 which leads to a quadrupolar moment when interacting with electric gradient fields. Such a coupling causes one central transition and two satellite transitions in ordered environments, such as human tissue. 60% of the NMR signal corresponds to the two satellite transitions and 40% of the signal originates from the central transition. Depending on the ^{23}Na ion binding, the transversal relaxation time (T_2) can result in two components. Within the tissue, the two satellite transitions result in a fast T_2 decay, whereas the central transition exhibits a slow T_2 decay (Bansal et al. 2000; Ra et al. 1986). The fact that 60% of the signal is fast decaying in human tissue makes ^{23}Na MRI challenging. Fast echo time and sophisticated acquisition methods are required, and achieving sufficient signal to noise is time consuming. That is why ^{23}Na MRI is still under development and mostly used in pre-clinical studies. The methodological developments have recently been reviewed (Konstandin and Nagel 2014; Madelin and Regatte 2013).

A few studies have already applied ^{23}Na MRI in skeletal muscle. For example, it has been shown that the tissue sodium concentration (TSC: defined as tissue ^{23}Na content per volume) increased by 34% ± 7% during one leg toe lift exercise (3–4 min) (Bansal et al. 2000) or hoped on one leg till fatigue 8–13% (2 ± 0.6 min) (Chang et al. 2010) compared to baseline. Furthermore, muscle disorders such as Duchenne's dystrophy or channelopathies are associated with increased TSC (Nagel et al. 2011; Weber et al. 2012).

Muscle wasting, at old age also called sarcopenia (Roubenoff 2000), is a physiological consequence of immobilization and unloading (Rittweger et al. 2005) and space flight (LeBlanc et al. 2000).

At least in young people, the disuse-related muscle atrophy is caused by shrinkage of muscle fibres (Narici and de Boer 2011). Thus, muscle atrophy is defined here as muscle volume loss and function loss. Since muscle fibres contain only little intracellular sodium, fibre shrinkage is expected to result in an increased relative portion of the extracellular Na rich compartment and, thus, in an increase in the apparent ^{23}Na concentration in MRI muscle scans. However, such changes in Na concentration in response to atrophy have not yet been assessed.

We have recently developed an exoskeleton that effectively unloads the mobilizing muscle group, the plantar flexor triceps surae muscles, as a model of localized muscle immobilization model (Weber et al. 2013). At the same time, this orthotic device leaves gait almost unaffected. Now, we have used this model in the NutriHEP study (clinical trials number NCT02698878) to test the effectiveness of a countermeasure intervention against muscle atrophy and insulin resistance (Zange et al. 2017). Here, we report on the ^{23}Na MRI data from this study.

We hypothesized an increase in sodium tissue concentration in the calf muscles due to unloading. This hypothesized effect should be explicable by shrinkage of muscle fibres. Accordingly, the secondary hypothesis was that the total ^{23}Na content within the muscle would be unaffected by the atrophy. Moreover, the water and fat composition in the muscle was hypothesized to change towards higher water content in the immobilized leg.

As a tertiary aim, we were interested in how atrophy induced by the Hephaistos orthosis would affect the fat/water constitution of skeletal muscle. This is because lack of physical activity and old age has been associated with in intramuscular fat accumulation as assessed by radiological techniques (Goodpaster et al. 2000). Contrary to the idea of increases fat content as a sign of muscle disuse, however, we had observed increases in muscular X-ray absorption in response to bed rest (Rittweger et al. 2013). As X-ray based approaches are not specific for the assessment of lipid content, other factors such as enrichment of intramuscular blood content could explain that observation. Thus, to further clarify whether there are changes in intramuscular lipid content as a result of immobilization, we also strived to assess muscular fat content in the present study.

Materials and methods

Subjects

Fourteen healthy male subjects were recruited for this study. All of these subjects completed the interventional protocol, but two of them failed to attend one or more MRI examinations and are, therefore, not included in the present analysis. The remaining 12 subjects had a mean age of 27.3 ± 3.9 years and a mean body mass index of

23.0 ± 1.54 kg/m^2 participated in the study. The study complied with the Declaration of Helsinki was approved by the ethics committee of the Ärztekammer Nordrhein, Düsseldorf, Germany, and all subjects had given their written informed consent before inclusion into the study. The study had been registered under clinical trials registration number NCT02698878 prior to commencement.

Study design

The NutriHEP was a randomized controlled interventional trial in an ambulatory setting. Muscle unloading was unilaterally provoked in all subjects in the lower leg musculature by wearing the HEPHAISTOS orthosis for 60 days. In addition to wearing the orthosis, seven subjects received a countermeasure using electrical muscle stimulation of the soleus muscle of the unloaded leg and a Lupin protein supplementation, while the remaining five subjects serve as a control without countermeasure.

The orthotic devices were manufactured and individually adapted by ORTEMA GmbH (Markgröningen, Germany). Volunteers wore the orthosis for 60 days under all daily circumstances from getting up in the morning until going to sleep in the night, but not during the night.

While the results relating to the countermeasure effectiveness have already been published (Zange et al. 2017), this part of the study is focussing on the relation between muscle volume changes and muscle sodium concentration.

MRI acquisition

MRI calf muscle acquisitions were obtained with a 3T scanner (mMR Biograph (PET-MRI scanner based on the Verio system), Siemens, Erlangen, Germany) with the scanner body coil and a mono-resonant sodium birdcage coil (Rapid Biomedical, Würzburg, Germany). The ^{23}Na coil has an 18 cm inner diameter and is equipped with a quadrature polarization on transmitting and receiving channel. Examinations were conducted 28 days before and on the 58th day of wearing the orthosis.

In the present analysis, we focus on TSC within lean muscle tissue. The examined muscles were the mobiliser muscles: medial and lateral gastrocnemius muscles, the soleus muscle, and the joint stabilizer muscles: the ventral muscle group (tibialis anterior, extensor digitorum longus, peroneus brevis, and peroneus longus muscles) and the central muscle group (flexor digitorum longus and tibialis posterior muscles). In this definition triceps, surae muscles work anti-gravitational (Adams et al. 2003) and all other muscles that are not attached to the achilles tendon are stabilizer (Sangwan et al. 2014).

MRI scans were obtained at rest and in supine position with an additional 30 min resting phase in supine position before the examinations to reach a constant distribution of the interstitial volume. First, the immobilized leg was positioned with the muscle belly at the most sensitive area of the ^{23}Na coil and the reference phantom beneath the lower leg. A wooden, individually configured footrest was used to ascertain reproducible positioning for each subject. After orthosis leg examination, the subject was repositioned in lying position for the control leg scan. The total testing time within the scanner room amounted to 50 min.

The literature is undetermined with regard to actual T_2 relaxation times for muscle tissue: Bansal et al. (2000) report 0.7–3.0 and 16–30 ms for the fast and slow components, respectively (Bansal et al. 2000), while Ra et al. (1986) suggest values of 0.5–8 and 15–30 ms, and Constantinides et al. (2000) report 0.46 ± 0.21 and 12.27 ± 1.94 ms for the fast and slow components (Constantinides et al. 2000). In aqueous sodium solutions, mono-exponential T_2 signal decay was found to be 20 ms or longer (Boada et al. 1994) or values were ranging from 30 to 50 ms (Ra et al. 1986), respectively. Another group found a strong temperature variance of T_2 signal decay in saline solutions 37–75 ms (2–50 °C) to 52 ms (21 °C) (Nagel et al. 2011).

In the intracellular compartment of skeletal muscles, typical sodium concentrations are 10–20 mmol/L. In the extracellular compartment, sodium concentration typically is 145 mmol/L. The extracellular compartment accounts for 10–15% of total muscle volume (Bansal et al. 2000). With this extracellular fraction, the total tissue sodium concentration in muscles is given in the range of 24.5–41.75 mmol/L. This is in agreement with Constantinides et al. (2000), who have reviewed the literature for tissue sodium concentrations determined from muscle biopsies and suggest 29.5 mmol/kg of wet weight ±2.4 as mean (Constantinides et al. 2000).

In consideration of the above, we acquired ^{23}Na MRI with a customized 2D gradient echo sequence similar to (Kopp et al. 2012) with the following parameter: frequency 32.602134 MHz, acquisition time (TA) 13:40 min, repetition time (TR) 100 ms, echo time (TE) 1.91 ms, flip angle 90 , average 128, and bandwidth 401 Hz/Px. The field of view (FoV) covered 192 × 192 mm with a 64 × 64 matrix which resulted in a resolution of 3 mm. The slice thickness was set to 30 mm.

For T_2 relaxometry, the gradient echo was repeated to obtain an echo train. Ten images at timepoints from 1.91 to 26.36 ms with a constant echo spacing of 2.73 ms were acquired.

For the assessment of muscle volume, water and fat contents a 2D proton density (PD)-weighted Dixon TSE (turbo spin echo) sequence was used with the following parameters: TA 2:48 min, TR 3000 ms, TE 11 ms, flip angle 180°, and bandwidth 292 Hz/Px. The FoV covered

192 × 192 mm with a 256 × 256 matrix which resulted in a resolution of 0.75 mm. The slice thickness is 5 mm with a gap of 5 mm in-between slices.

Sodium coil excitation homogeneity was controlled by a saline water probe that filled out the coil diameter.

Muscle volume analysis

The 17 slices that were acquired (^{1}H TSE) from the calf muscle belly were utilized for muscle segmentation and subsequent volume estimation. The following calf muscles were differentiated (Fig. 1): medial gastrocnemius muscle, lateral gastrocnemius muscle, soleus muscle, ventral muscle group, and central muscle group. The muscle volumes were estimated by multiplying the segmented muscle area from the 17 slices with the slice thickness.

Tissue sodium concentration analysis

TSC was determined by comparison with the external reference phantoms that contained 10, 20, 30, and 40 mmol/L NaCl solutions (Kopp et al. 2012). For registration of ^{23}Na and ^{1}H scans, image orientation was transversal in the magnets' isocenter. The FoV covered the same area, which allowed transposing the regions of interest (ROI) of the above-mentioned muscle segmentations to the ^{23}Na images. A linear model was calculated from ROIs of the reference phantom tubes for the calibration of the muscle tissue concentration. Vessels and skin tissue are sodium rich; these high intensity peaks were excluded in the segmentation. Delta TSC values resulted by subtracting post period from baseline TSC values.

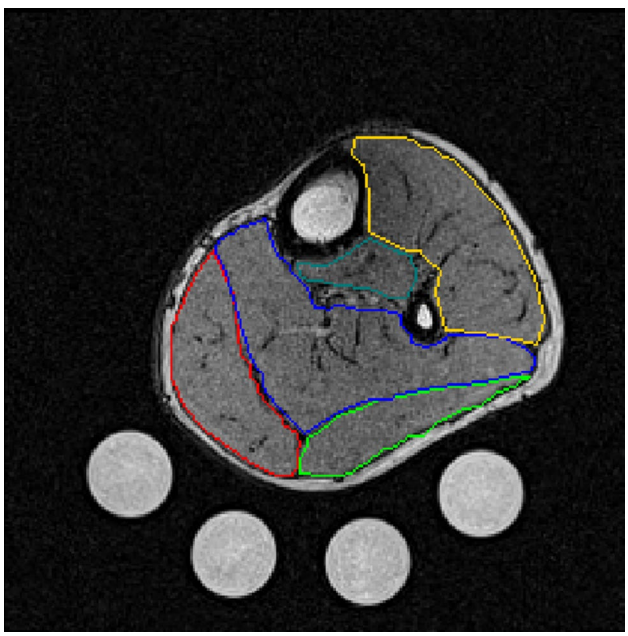

Fig. 1 Muscle segmentation of orthosis leg baseline acquisition with Dixon TSE opposed phase image: m. gastrocnemius med. (*red*), m. gastrocnemius lat. (*light green*), m. Soleus (*blue*), ventral muscle group (*yellow*), and central muscle group (*cyan*) (color figure online)

Sodium content in mmol was calculated by multiplication of the TSC in mmol/L with the analysed muscle volume in litres.

Signal-to-noise ratio was calculated according to SNR = *S*/*N*, where *S* is the mean signal intensity from muscle tissue and *N* is the standard deviation of background noise. The mean SNR of the ^{23}Na MRI in muscle tissue was 7.61 ± 0.69. To measure the reproducibility of our outcome variables, we repeated measurements on a phantom 40 times. The phantom had a known aqueous sodium solution of 14 mmol/L. The estimated concentration is 13.37 ± 0.6 mmol/L.

Sodium T_2^* relaxomtery

Sodium T_2^* signal decay was derived from muscle ROIs of medial and lateral gastrocnemius, soleus, ventral muscle group, and the central muscle group. For sufficient signal-to-noise ratio, the mean signal intensity of the voxels from all muscles was used. The noise offset from image background was subtracted from the signal intensity.

For the T_2^* signal decay in the phantom aqueous sodium solution, a mono-exponential fitting function (1) was utilized with three parameters:

$$F(\mathrm{TE}) = S_0 \times \mathrm{e}^{-\frac{\mathrm{TE}}{T_{2*}}} + S_1, \tag{1}$$

with S_0 signal intensity sodium solution, T_2^* relaxation time, and S_1 offset which is caused by noise.

For muscle tissue, a bi-exponential fitting function (2) was used with five parameters:

$$F(\mathrm{TE}) = S_0 \times \mathrm{e}^{-\frac{\mathrm{TE}}{T_{2*\_\mathrm{f}}}} + S_1 \times \mathrm{e}^{-\frac{\mathrm{TE}}{T_{2*\_\mathrm{s}}}} + S_3, \tag{2}$$

with S_0 signal intensity from the fast decaying component S_1 signal intensity from the slow decaying component, $T_{2\_\mathrm{f}}^*$ relaxation time of the fast decaying component, $T_{2\_\mathrm{s}}^*$ relaxation time of the slow decaying component, and S_3 offset which is caused by noise.

The fraction of the fast (F_f) and slow (F_s) decaying T_2^* components is calculated with the following formulas (3) and (4):

$$F_\mathrm{f} = 100 \times S_0/(S_0 + S_1) \tag{3}$$

$$F_\mathrm{s} = 100 \times S_1/(S_0 + S_1). \tag{4}$$

To determine the mono and bi-exponential fit function, a multidimensional unconstrained nonlinear minimization (Nelder–Mead) was utilized in MATLAB (Release 2012b,

The MathWorks, Inc., Natick, MA, USA). The ordinary least squares cost function $\sum(F(\mathrm{TE}_i) - y((\mathrm{TE}_i))^2$ was solved with randomly chosen starting values to avoid local minima solutions. The optimization was repeated 10,000 times and the solution with the highest R^2 value was chosen.

Fat and water fraction analyses

The fat and water fractions were assessed by the pixel signal intensities of the in-phase water and in-phase fat DIXON images according to the following formulas (5) and (6) (Fischer et al. 2014):

$$\text{Water fraction (WF)} = \mathrm{SI}_{\mathrm{water}}/(\mathrm{SI}_{\mathrm{fat}} + \mathrm{SI}_{\mathrm{water}}) \quad (5)$$

$$\text{Fat fraction (FF)} = \mathrm{SI}_{\mathrm{fat}}/(\mathrm{SI}_{\mathrm{fat}} + \mathrm{SI}_{\mathrm{water}}). \quad (6)$$

Statistics

All statistical analyses were performed with IBM SPSS (V.21, Chicago, IL). Group mean values with their SD were calculated for each muscle of interest.

Linear mixed-effects (LME) models were constructed with period (baseline: pre immobilization vs. post: state end of orthosis period), leg (control leg vs. orthosis leg), and group (control vs. countermeasure) as fixed effects, and with subject as random effect. All possible interactions (including three-way) were included in the initial models. Model simplification strategy then started with elimination of the three-way interaction. Normally distributed residuals were required for model acceptance. Significance was assumed at $P < 0.05$. Moreover, normal distribution of the raw data was verified by Kolmogorov–Smirnov test.

Two-tailed t test was utilized after LME to follow up on significant ANOVA effects. Pearson correlation (r) was used to test for a relationship between changes in muscle volume and sodium content.

Results

TSC and sodium content, as well as changes over time in these variables were comparable between the two subject groups for all muscles (medial gastrocnemius $P = 0.176$; other muscles $P > 0.26$). Therefore, the control subjects and training subjects were lumped together in the subsequent statistical analyses and are reported as one group in the following.

^{23}Na tissue sodium concentration (TSC)

TSC increased from baseline to post period in the orthosis leg, whereas no significant changes occurred for TSC in the control leg. Detailed LME statistical analysis of TSC is given in Table 1. ^{23}Na MRI results from the baseline and post acquisitions of calf cross section are depicted in Fig. 2 for the orthosis leg.

Testing TSC (Table 2) with paired t test revealed an increase from baseline to post period in all muscle groups of the orthosis leg. Predominantly, TSC increased in triceps surae muscles, namely, by 17.4 ± 16.8% [$t(11) = -3.553$, $P = 0.05$] in the medial gastrocnemius muscle, by 11.1 ± 12.5% [$t(11) = -2.366$, $P = 0.037$] in the lateral gastrocnemius muscle, and by 16.2 ± 4.7% [$t(11) = -11.221$, $P < 0.001$] in the soleus muscle. TSC increased to a lesser extent in the ventral muscle group by 10.0 ± 10.5% [$t(11) = -3.160$, $P = 0.009$] and in the central muscle group by 10.7 ± 10.0% [$t(11) = -3.831$, $P = 0.003$]. The delta TSC percentage values for the orthosis and control leg are depicted in Fig. 3.

LME analysis of the sodium content found effects of period and of leg in the mobilizer muscle group and ventral muscle group only (Table 3). The paired t test revealed an 17.7 ± 23.08% increase of sodium content (Table 4) in the lateral gastrocnemius muscle in the control leg [$t(11) = -2.970$, $P = 0.013$] from baseline to post period. In the orthosis leg, the sodium content increased by 10.4 ± 12.3% in the muscle group of the ventral muscle group [$t(11) = -3.027$, $P = 0.012$].

Muscle volume

LME revealed period and leg effects in the calf muscle volume (Table 5). Muscle volume (Table 6) decreased

Table 1 TSC LME statistical analysis with the fixed effects period: baseline (pre immobilization) and post (end of orthosis period), the leg: control leg and orthosis leg, and the group: control subjects and training subjects with electrostimulation and the interaction between fixed effects

Muscle	Fixed effect	F value	P value
m. gastrocnemius med.	Leg	$F(1, 31) = 13.123$	0.001
	Period	$F(1, 31) = 6.392$	0.017
	Leg × period	$F(1, 31) = 8.046$	0.008
	Leg × group	$F(1, 31) = 4.644$	0.039
m. gastrocnemius lat.	Leg	$F(1, 31) = 10.981$	0.002
m. soleus	Leg	$F(1, 31) = 10.443$	0.003
	Period	$F(1, 31) = 39.638$	<0.001
	Leg × period	$F(1, 31) = 13.770$	0.001
	Leg × group	$F(1, 31) = 5.150$	0.030
Ventral muscle group	Period	$F(1, 31) = 3.412$	0.074
	Leg × period	$F(1, 31) = 5.125$	0.031
Central muscle group	Period	$F(1, 31) = 3.476$	0.072
	Leg × period	$F(1, 31) = 3.317$	0.078

However, some interaction with the fixed effect group was found, no sole significance occurred in the fixed effect group in any muscle

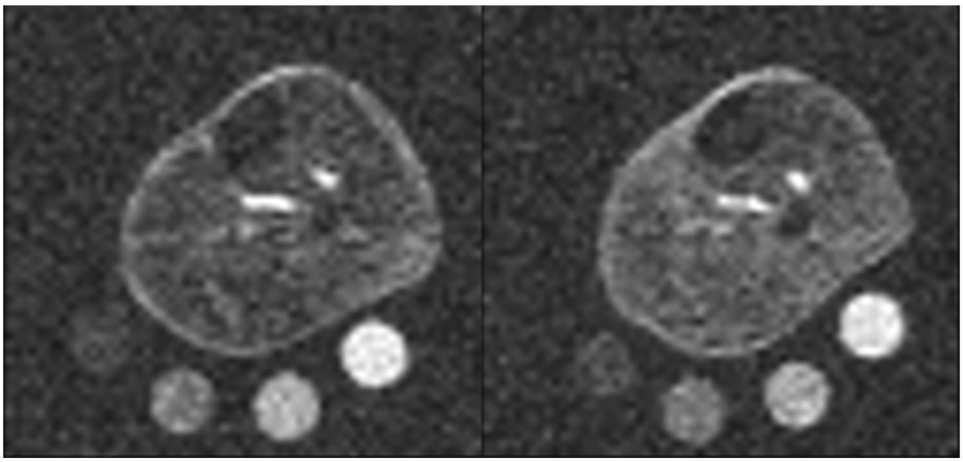

Fig. 2 Pre and end of orthosis period ^{23}Na MRI acquisition of the orthosis leg at the calf. Reference phantoms beneath the leg appear in different intensities due to its sodium concentration (from *left* to *right*: 10, 20, 30, and 40 mmol/L NaCl solutions)

Table 2 Tissue sodium concentration (TSC) given in mmol/L for the analysed muscles of the control and orthosis leg during baseline and after 60 days intervention

Muscle	Leg	TSC baseline (mmol/L)	TSC post (mmol/L)
m. gastrocnemius med.	Control	11.2 ± 1.7	11.2 ± 1.1
	Orthosis	11.6 ± 2.2	13.5 ± 2.4 *
m. gastrocnemius lat.	Control	11.3 ± 2.4	11.2 ± 1.7
	Orthosis	12.1 ± 3.6	13.2 ± 3.1 *
m. soleus	Control	13.5 ± 1.7	14.0 ± 1.3
	Orthosis	13.3 ± 1.1	15.5 ± 1.5 *
Ventral muscle group	Control	11.9 ± 1.1	11.8 ± 0.9
	Orthosis	11.4 ± 1.1	12.5 ± 1.4 *
Central muscle group	Control	11.5 ± 1.5	11.5 ± 1.1
	Orthosis	11.2 ± 1.2	12.3 ± 1.4 *

Countermeasures revealed no effect on TSC; therefore, the countermeasure group and control group were put together

* Significance ($P < 0.05$) assessed by a paired t test from baseline to post period

in the orthosis leg in the medial gastrocnemius muscle by −5.4 ± 8.3% [$t(11) = 2.292$, $P = 0.043$, see Fig. 4] and by −7.8 ± 15.0% [$t(11) = 2.283$, $P = 0.043$] in the soleus muscle.

In the control leg, however, muscle volume increased by +6.9 ± 9.1% [$t(11) = -2.488$, $P = 0.03$] in the lateral gastrocnemius muscle, whereas it decreased by −4.7 ± 5.0% in the soleus muscle [$t(11) = 3.120$, $P = 0.01$] volume.

Notably, and as previously reported (Zange et al. 2017), muscle volume changes differed between the groups (control and exercise group) as for the soleus muscle but not for any other group.

A positive linear correlation was found between delta sodium content and delta muscle volume was found for the medial gastrocnemius muscle in the orthosis leg: ($r = 0.788$, $P = 0.002$) and in ventral muscle group in the control leg: ($r = 0.599$, $P = 0.04$) and a negative linear correlation in the orthosis leg: ($r = -0.608$, $P = 0.036$).

Fat and water fractions in muscle tissue

LME revealed a leg effect for the soleus muscle [$F(1, 31) = 5.846$, $P = 0.022$], for the central muscle group [$F(1, 31) = 4.458$, $P = 0.043$], and a trend for the medial gastrocnemius muscle [$F(1, 31) = 3.917$, $P = 0.057$]. No group effect occurred in any muscle. Fat fraction (Table 7) decreased in the orthosis leg, as evidenced by paired t test [$t(11) = 2.338$, $P = 0.039$] by −0.54 ± 0.81% in the lateral gastrocnemius muscle, [$t(11) = 3.451$, $P = 0.005$] by −0.42 ± 0.42% in the ventral muscle group, and [$t(11) = 4.133$, $P = 0.002$] by −0.63 ± 0.53% in the central muscle group. No significant changes were found in the control leg. The statistical evaluation of the water fraction yielded effects that were reciprocal to the fat fraction results.

Sodium T_2^* relaxation time

T_2^* relaxation times (Table 8) and fraction did not change significantly from baseline to post period. No interaction with LME between the fixed factor leg, period, and group occurred.

The echo train acquisition of the saline water probe from homogeneity testing resulted in a mono-exponential decay of 43.3 ms ± 1.82 ms (R^2: 0.9749 ± 0.0027).

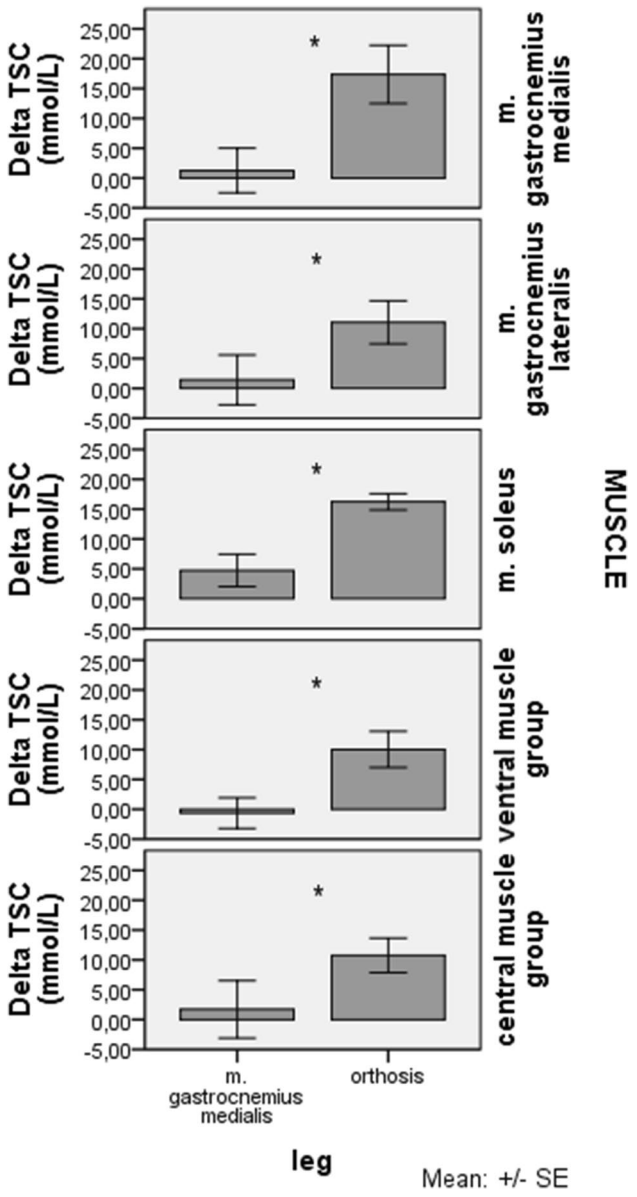

Fig. 3 Delta TSC from baseline to post period in muscle tissue of interest in control and orthosis leg. ^{23}Na MRI revealed elevated TSC in all muscle groups in post period in orthosis leg. No changes can be found in TSC in the control leg. The *asterisk* indicates significance ($P < 0.05$) assessed by a paired *t* test from baseline to post period

Table 3 Sodium content LME statistical analysis with the fixed effects period: baseline (pre immobilization) and post (end of orthosis period), the leg: control leg and orthosis leg, and the group: control subjects and training subjects with electrostimulation and the interaction between fixed effects

Muscle	Fixed effect	*F* value	*P* value
m. gastrocnemius med.	Leg	$F(1, 31) = 9.261$	0. 005
m. gastrocnemius lat.	Period	$F(1, 31) = 4.776$	0. 037
Ventral muscle group	Period	$F(1, 31) = 4.484$	0. 042

Discussion

The major finding of this ^{23}Na-MRI study was an increase in the sodium concentration in lower leg musculature after 60 days of wearing the Hephaistos orthosis. Tissue sodium concentration is generally understood as the ^{23}Na content measured volumetrically, and thus, content per volume is concentration. However, whereas the sodium concentration was clearly increased, its content was generally un-changed. One might conclude from this that the observed increases in concentration merely resulted from the reduction in distribution volume that is associated with the immobilization-induced muscle atrophy. This would fit to our hypothesis that the low sodium intracellular compartment of the muscle fibres was shrinking, while the sodium rich extracellular space remains almost constant.

The observed increases in TSC occurred quite generally throughout the whole lower leg musculature in the orthosis leg. They were most pronounced (~15%) in the mobilizer muscle group, but were also present (~10%) in the ventral muscle group and the central muscle group. The changes found are in the range of clinical relevance, i.e., sodium concentration of muscle tissue after dialysis (Dahlmann et al. 2015) and muscle TSC in hypertensive patients (Kopp et al. 2013). This leads to the rationale that the increases in TSC were mainly caused by muscle atrophy by wearing the orthosis. In addition, a change in the ratio of extracellular vs. intracellular volume likely occurred and sodium concentration increased correspondingly in at least one of the two compartments. The utilized method is not capable of distinguishing the origin of the sodium concentration or content. For further investigations regarding the signal origin (intra- or extracellular space), advanced tools such as tipple quantum filtering could be used to identify signal from the intracellular compartment (Allis et al. 1991), though low SNR is a big issue.

It is known that muscle atrophy results in muscle cell shrinking mainly by intracellular protein loss. On the one side, intracellular sodium concentration should increase by osmotic pressure; on the other side, the sodium potassium pump keeps the intracellular sodium concentration constant in a narrow band. The question is when this mechanism gets out of kilter, which is in particular interesting for pathophysiology and early stage detections. Notably, it is hypothesized that a reduced nerve drive is the cause for less rate of force development in elderly (Aagaard et al. 2010). A disturbed intra- and extracellular sodium balance would affect the development of action potential that would be in consistence with the aforementioned hypothesis. The effect of extracellular and intracellular volume shifts was likely largest

Table 4 Sodium content in the whole section of an analysed muscle given in mmol of the control and orthosis leg during baseline and after 60 day intervention

Muscle	Leg	Sodium content baseline (mmol)	Sodium content post (mmol)
m. gastrocnemius med.	Control	0.385 ± 0.15	0.392 ± 0.13
	Orthosis	0.420 ± 0.15	0.455 ± 0.14
m. gastrocnemius lat.	Control	0.179 ± 0.07	0.200 ± 0.06*
	Orthosis	0.183 ± 0.07	0.204 ± 0.08
m. soleus	Control	0.829 ± 0.19	0.827 ± 0.20
	Orthosis	0.824 ± 0.16	0.853 ± 0.24
Ventral muscle group	Control	0.503 ± 0.09	0.507 ± 0.07
	Orthosis	0.499 ± 0.07	0.551 ± 0.09*
Central muscle group	Control	0.141 ± 0.03	0.146 ± 0.04
	Orthosis	0.140 ± 0.05	0.144 ± 0.04

* Significance ($P < 0.05$) assessed by a paired t test from baseline to post period

Table 5 Muscle volume LME statistical analysis with the fixed effects period: baseline (pre immobilization) and post (end of orthosis period), the leg: control leg and orthosis leg, and the group: control subjects and training subjects with electrostimulation and the interaction between fixed effects

Muscle	Fixed effect	F value	P value
m. gastrocnemius med.	Period	$F(1, 31) = 4.223$	0.048
m. gastrocnemius lat.	Leg	$F(1, 31) = 6.560$	0.016
	Leg × period	$F(1, 31) = 4.426$	0.044
m. soleus	Period	$F(1, 31) = 10.771$	0.003

Table 6 Calf muscle volumes estimated from 17 slices with a inter slice gap of 5 mm and a 5 mm slice thickness in the orthosis and control leg during the baseline and at the end of orthosis period

Muscle	Leg	Volume baseline (ml)	Volume post (ml)
m. gastrocnemius med.	Control	113.0 ± 33.0	113.2 ± 31.2
	Orthosis	116.1 ± 31.4	109.0 ± 27.2*
m. gastrocnemius lat.	Control	60.7 ± 19.9	64.1 ± 19.9*
	Orthosis	59.8 ± 21.6	55.8 ± 21.0
m. soleus	Control	205.9 ± 31.9	195.9 ± 29.7*
	Orthosis	208.7 ± 29.0	190.9 ± 30.5*
Ventral muscle group	Control	138.5 ± 14.8	140.2 ± 14.2
	Orthosis	142.7 ± 16.6	141.1 ± 17.3
Central muscle group	Control	47.1 ± 10.8	47.6 ± 8.3
	Orthosis	47.4 ± 12.9	44.7 ± 11.5*

* Significance ($P < 0.05$) assessed by a paired t test from baseline to post period

in those mobilizer muscle group treated by the orthosis and the electrostimulation countermeasure. Nevertheless, extracellular and intravascular fluid changes may not be excluded from the variable sodium signal patterns found in both intramuscular tissue structures but also in the vascular space. Interestingly, mobilizer muscles treated by orthosis only showed a significant loss in strength, whereas the corresponding muscle group additionally treated by electrostimulation did not lose strength (Zange et al. 2017). Therefore, the increase in sodium concentration by unloading in the orthosis likely did not affect muscle contraction.

Another influencing aspect on TSC is the microvascular adaptation, which can occur as a result of muscle unloading and electrostimulation (Hudlicka 1985). Potentially, the capillary density may increase by these factors and lead to increased blood volume. Blood is sodium rich (~140 mMol/L) and thus would increase the apparent sodium concentration of a muscle. TSC values for the training group were not different from the control group and were pooled together. Thus, electrostimulation seems to have a negligible effect on TSC. The muscular water amount did not or changed only slightly, which excludes water accumulation and makes big blood volumes unlikely. In this study, we can exclude influence of capillarization on TSC. Histological analysis revealed no difference in capillary density and the average capillaries per fibre ratio between baseline and unloading biopsy samples. The details will be published separately. The general influence of capillary density increase on TSC in the musculature needs further investigation.

The present results also help to better understand the nature of the increased muscle x-ray attenuation after bed rest. First, the fact that the water and fat fractions were increasing and decreasing, respectively (albeit by a small amount), support the notion of decreased intramuscular lipid concentration as a result of immobilization (Desplanches et al. 1998), at least in young people. It had been speculated that bed rest-related fluid shifts might also be involved in increased leg muscle X-ray attenuation (Rittweger et al. 2013). The present result is

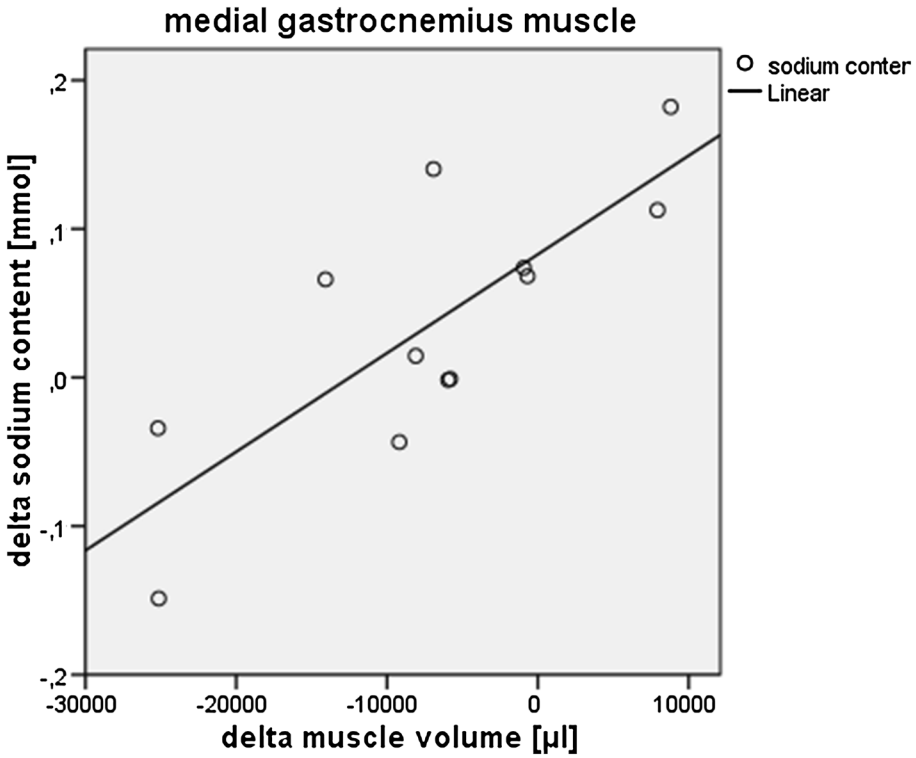

Fig. 4 Positive linear correlation between delta sodium content and delta volume in medial gastrocnemius muscle in the orthosis leg was found

Table 7 Baseline and end of orthosis period fat fraction in the calf muscles obtained from the 17 slice DIXON acquisition in the orthosis and control leg

Muscle	Leg	Fat fraction baseline (%)	Fat fraction post (%)
m. gastrocnemius med.	Control	10.7 ± 1.2	10.6 ± 1.3
	Orthosis	10.2 ± 1.2	9.9 ± 1.2
m. gastrocnemius lat.	Control	10.8 ± 0.9	10.6 ± 0.8
	Orthosis	10.8 ± 1.4	10.3 ± 1.0*
m. soleus	Control	10.8 ± 1.7	10.7 ± 1.7
	Orthosis	10.9 ± 1.5	11.2 ± 2.0
Ventral muscle group	Control	10.2 ± 1.4	10.0 ± 1.3
	Orthosis	10.8 ± 0.8	10.4 ± 0.9*
Central muscle group	Control	10.1 ± 1.5	9.7 ± 1.4
	Orthosis	10.9 ± 0.9	10.3 ± 0.9*

* Significance ($P < 0.05$) assessed by a paired t test from baseline to post period

compatible with that notion, and they demonstrate that the question could be addressed by combined ^{23}Na and fat imaging in a bed rest scenario.

The present data also offer space for some methodological considerations about ^{23}Na imaging. The T_2^* fraction finding, estimated by the relaxation fit, seems consistent with 60% signal intensity from the satellite transitions in ordered tissue and T_2^* relaxation times are in the range of the literature (Bansal et al. 2000; Constantinides et al. 2000; Ra et al. 1986). On contrary to T_2, T_2^* relaxation times are affected by magnetic field inhomogeneities and are, therefore, lower. As the slow and fast decaying T_2^* fractions depend on the tissue composition (Berendsen and Edzes 1973), changes in the tissue composition could alter the fraction (Rooney and Springer 1991; Shinar and Navon 1986). However, this fraction was comparable between baseline and end of orthosis phase. This finding should be considered critically. The method used to determine the fast T_2^* component is in-appropriate, because the first TE is in range of the expected T_2^* value. This results in high standard deviations in the fast decaying component and in the fraction values. Nevertheless, the slow decaying component is still valuable though not sensitive enough in this case.

This study has more limitations. The determination of TSC is not given in absolute quantitative values. TSC quantification is a rather relative comparison between baseline and end of orthosis values. T_2 effects lead to signal loss which vanishes faster in tissue than in water solutions. Moreover, the calibration phantom gives signal from watery diluted sodium, which provides a relative comparison of signal intensities only. As an aqueous solution, the reference phantoms are lacking a fast T_2 component. Due to its spin, 3/2 sodium has a bi-exponential

Table 8 Fast and slow sodium T_2^* relaxation times and their fraction from calf muscle tissue

Leg	Fast T_2^* (ms)	Slow T_2^* (ms)	Fast T_2^* fraction (%)	Slow T_2^* fraction (%)	Fit correlation R^2
Baseline control leg	1.41 ± 0.74	11.51 ± 2.8	62.1 ± 14.2	37.9 ± 14.2	0.9987 ± 0.00087
Baseline orthosis leg	1.71 ± 0.85	13.25 ± 3.3	60.5 ± 10.9	39.6 ± 10.9	0.9982 ± 0.00119
Post control leg	1.23 ± 0.59	11.07 ± 2.27	62.8 ± 14.0	37.2 ± 14.0	0.9987 ± 0.00089
Post orthosis leg	1.38 ± 0.6	11.6 ms ± 2.8 ms	62.0 ± 10.2	38.0 ± 10.2	0.9992 ± 0.00057

transversal relaxation T_2 decay in biological tissue. Therefore, sequences with short echo times (TE) and appropriate acquisition techniques are necessary for the acquisition of both components. Different sequences result in different sodium concentrations estimated in healthy subjects: 28.4 ± 3.6 mmol/kg of wet weight (Constantinides et al. 2000), 18.9 ± 1.9 mmol/L (Kopp et al. 2012) and 24 ± 2 mmol/L (Nagel et al. 2011) all in the calf muscle tissue. One reason for this is the different TE and acquisition strategy used. Here, we used a rather long TE, which is not capable of capturing the entire fast T_2 component and, therefore, mainly allows conclusions about the concentration of water dissolved sodium. The quantification of saline water probe is slightly underestimated by less than 5%.

A more striking argument why prior published TSC values might differ is that none of the compared publications stated how long the subjects or patients rested in lying position for water equilibrium before the examination. In this study, subjects rested 30 min in supine position. This leads to less extracellular fluid amount in the lower body. The extracellular fluid mainly contributes to the TSC signal, and thus, less fluid might result in lower overall muscle TSC.

All in all, ^{23}Na MRI is a considerable challenging method for sodium detection. ^{23}Na MRI suffers from poor signal resolution, large voxel size, and long acquisition times (Bangerter et al. 2016).

Conclusion

In conclusion, the ^{23}Na MRI approach chosen in this study is sensitive enough to find an increase in muscle TSC after 60 days of muscle unloading. This effect of wearing the orthosis was only gradually different between the mobilizer muscle group and the other muscles in the lower leg. Furthermore, the increase in TSC was not affected by electrostimulation of triceps surae muscles in the countermeasure group. Therefore, further examinations are needed to study the underlying mechanism. Nevertheless, quantifying sodium could become a promising indicator for early non-invasive diagnosis of muscle pathologies.

For future physiological studies on muscle wasting, a more frequent sampling of the subjects could be performed. To overcome the problem of acquiring the fast transversal T_2 decay techniques such as the density-adapted three-dimensional radial projection reconstruction (DA-3DPR) (Nagel et al. 2009), the flexible twisted projection imaging (flexTPI) (Lu et al. 2010) should be performed. These pulse sequences were capable of very fast echo times by a radial sampling of the *k* space.

Acknowledgements K. Schopen received a Helmholtz Space Life Sciences Research School (SpaceLife) Ph.D. scholarship. SpaceLife was funded in equal parts by the Helmholtz Association (Grant No.: VH-KO-300) and the German Aerospace Center (DLR). The Nutri-HEP study was funded by the DLR internal cost object 2475 101.

Compliance with ethical standards

Ethical approval All procedures performed in studies involving human participants were in accordance with the ethical standards of the institutional and/or national research committee and with the 1964 Helsinki declaration and its later amendments or comparable ethical standards.

Conflict of interest The authors declare that they have no conflict of interest.

References

Aagaard P, Suetta C, Caserotti P, Magnusson SP, Kjaer M (2010) Role of the nervous system in sarcopenia and muscle atrophy with aging: strength training as a countermeasure. Scand J Med Sci Sports 20:49–64. doi:10.1111/j.1600-0838.2009.01084.x

Adams GR, Caiozzo VJ, Baldwin KM, (2003) Skeletal muscle unweighting: spaceflight and ground-based models. J Appl Physiol 95(6):2185–2201

Allis JL, Seymour A-ML, Radda GK (1991) Absolute quantification of intracellular Na^+ using triple-quantum-filtered sodium-23 NMR. J Magn Reson (1969) 93:71–76. doi:10.1016/0022-2364(91)90032-o

Bangerter NK, Tarbox GJ, Taylor MD, Kaggie JD (2016) Quantitative sodium magnetic resonance imaging of cartilage, muscle, and tendon. Quant Imaging Med Surg 6:699–714. doi:10.21037/qims.2016.12.10

Bansal N, Szczepaniak L, Ternullo D, Fleckenstein JL, Malloy CR (2000) Effect of exercise on ^{23}Na MRI and relaxation characteristics of the human calf muscle. J Magn Reson Imaging 11:532–538. doi:10.1002/(sici)1522-2586(200005)11:5<532:aid-jmri9>3.0.co;2-#

Berendsen HJC, Edzes HT (1973) The observation and general interpretation of sodium magnetic resonance in biological material.

Ann N Y Acad Sci 204:459–485. doi:10.1111/j.1749-6632.1973.tb30799.x

Boada FE, Christensen JD, Huang-Hellinger FR, Reese TG, Thulborn KR (1994) Quantitativein vivo tissue sodium concentration maps: the effects of biexponential relaxation. Magn Reson Med 32:219–223. doi:10.1002/mrm.1910320210

Borthakur A, Shapiro EM, Beers J, Kudchodkar S, Kneeland JB, Reddy R (2000) Sensitivity of MRI to proteoglycan depletion in cartilage: comparison of sodium and proton MRI osteoarthritis and cartilage/OARS. Osteoarthr Res Soc 8:288–293. doi:10.1053/joca.1999.0303

Borthakur A, Mellon E, Niyogi S, Witschey W, Kneeland JB, Reddy R (2006) Sodium and T1rho MRI for molecular and diagnostic imaging of articular cartilage. NMR Biomed 19:781–821. doi:10.1002/nbm.1102

Chang G, Wang L, Schweitzer ME, Regatte RR (2010) 3D 23Na MRI of human skeletal muscle at 7 Tesla: initial experience. Eur Radiol 20:2039–2046. doi:10.1007/s00330-010-1761-3

Constantinides CD, Gillen JS, Boada FE, Pomper MG, Bottomley PA (2000) Human skeletal muscle: sodium MR imaging and quantification-potential applications in exercise and disease. Radiology 216:559–568. doi:10.1148/radiology.216.2.r00jl46559

Dahlmann A et al (2015) Magnetic resonance-determined sodium removal from tissue stores in hemodialysis patients. Kidney Int 87:434–441. doi:10.1038/ki.2014.269

Desplanches D, Hoppeler H, Mayet MH, Denis C, Claassen H, Ferretti G (1998) Effects of bedrest on deltoideus muscle morphology and enzymes. Acta Physiol Scand 162:135–140. doi:10.1046/j.1365-201X.1998.0288f.x

Drummer C, Hesse C, Baisch F, Norsk P, Elmann-Larsen B, Gerzer R, Heer M (2000) Water and sodium balances and their relation to body mass changes in microgravity. Eur J Clin Investig 30:1066–1075. doi:10.1046/j.1365-2362.2000.00766.x

Fischer MA, Pfirrmann CW, Espinosa N, Raptis DA, Buck FM (2014) Dixon-based MRI for assessment of muscle-fat content in phantoms, healthy volunteers and patients with achillodynia: comparison to visual assessment of calf muscle quality. Eur Radiol 24:1366–1375. doi:10.1007/s00330-014-3121-1

Goodpaster BH, Kelley DE, Thaete FL, He J, Ross R (2000) Skeletal muscle attenuation determined by computed tomography is associated with skeletal muscle lipid content. J Appl Physiol 89:104–110

Hudlicka O (1985) Development and adaptability of microvasculature in skeletal muscle. J Exp Biol 115:215–228

Inglese M et al (2010) Brain tissue sodium concentration in multiple sclerosis: a sodium imaging study at 3 tesla. Brain: J Neurol 133:847–857. doi:10.1093/brain/awp334

Konstandin S, Nagel AM (2014) Measurement techniques for magnetic resonance imaging of fast relaxing nuclei. Magma 27:5–19. doi:10.1007/s10334-013-0394-3

Kopp C et al (2012) (23)Na magnetic resonance imaging of tissue sodium. Hypertension 59:167–172. doi:10.1161/HYPERTENSIONAHA.111.183517

Kopp C et al (2013) ^{23}Na magnetic resonance imaging-determined tissue sodium in healthy subjects and hypertensive patients. Hypertension 61:635–640. doi:10.1161/HYPERTENSIONAHA.111.00566

LeBlanc A et al (2000) Muscle volume, MRI relaxation times (T2), and body composition after spaceflight. J Appl Physiol 89:2158–2164

Lu A, Atkinson IC, Claiborne TC, Damen FC, Thulborn KR (2010) Quantitative sodium imaging with a flexible twisted projection pulse sequence. Magn Reson Med 63:1583–1593. doi:10.1002/mrm.22381

Maarouf A et al (2014) Topography of brain sodium accumulation in progressive multiple sclerosis. Magma 27:53–62. doi:10.1007/s10334-013-0396-1

Madelin G, Regatte RR (2013) Biomedical applications of sodium MRI in vivo. J Magn Reson Imaging: JMRI 38:511–529. doi:10.1002/jmri.24168

Nagel AM, Laun FB, Weber MA, Matthies C, Semmler W, Schad LR (2009) Sodium MRI using a density-adapted 3D radial acquisition technique. Magn Reson Med 62:1565–1573. doi:10.1002/mrm.22157

Nagel AM, Amarteifio E, Lehmann-Horn F, Jurkat-Rott K, Semmler W, Schad LR, Weber MA (2011) 3 Tesla sodium inversion recovery magnetic resonance imaging allows for improved visualization of intracellular sodium content changes in muscular channelopathies. Investig Radiol 46:759–766. doi:10.1097/RLI.0b013e31822836f6

Narici MV, de Boer MD (2011) Disuse of the musculo-skeletal system in space and on earth. Eur J Appl Physiol 111:403–420. doi:10.1007/s00421-010-1556-x

Ooms KJ, Cannella M, Vega AJ, Marcolongo M, Polenova T (2008) ^{23}Na TQF NMR imaging for the study of spinal disc tissue. J Magn Reson 195:112–115. doi:10.1016/j.jmr.2008.07.024

Ouwerkerk R, Bleich KB, Gillen JS, Pomper MG, Bottomley PA (2003) Tissue sodium concentration in human brain tumors as measured with ^{23}Na MR imaging. Radiology 227:529–537. doi:10.1148/radiol.2272020483

Paling D et al (2013) Sodium accumulation is associated with disability and a progressive course in multiple sclerosis. Brain: J Neurol 136:2305–2317. doi:10.1093/brain/awt149

Ra JB, Hilal SK, Cho ZH (1986) A method forin vivo MR imaging of the shortT2 component of sodium-23. Magn Reson Med 3:296–302. doi:10.1002/mrm.1910030213

Rittweger J, Frost HM, Schiessl H, Ohshima H, Alkner B, Tesch P, Felsenberg D (2005) Muscle atrophy and bone loss after 90 days' bed rest and the effects of flywheel resistive exercise and pamidronate: results from the LTBR study. Bone 36:1019–1029. doi:10.1016/j.bone.2004.11.014

Rittweger J, Moller K, Bareille MP, Felsenberg D, Zange J (2013) Muscle X-ray attenuation is not decreased during experimental bed rest. Muscle Nerve 47:722–730. doi:10.1002/mus.23644

Rooney WD, Springer CS (1991) A comprehensive approach to the analysis and interpretation of the resonances of spins 3/2 from living systems. NMR Biomed 4:209–226. doi:10.1002/nbm.1940040502

Roubenoff R (2000) Sarcopenia and its implications for the elderly. Eur J Clin Nutr 54:S40–S47. doi:10.1038/sj.ejcn.1601024

Sangwan S, Green RA, Taylor NF (2014) Characteristics of Stabilizer Muscles: a Systematic Review. Physiother Can 66(4):348–358

Shinar H, Navon G (1986) Sodium-23 NMR relaxation times in body fluids. Magn Reson Med 3:927–934. doi:10.1002/mrm.1910030613

Titze J et al (2003) Osmotically inactive skin Na^+ storage in rats. Am J Physiol Renal Physiol 285:F1108–F1117. doi:10.1152/ajprenal.00200.2003

Weber MA, Nagel AM, Wolf MB, Jurkat-Rott K, Kauczor HU, Semmler W, Lehmann-Horn F (2012) Permanent muscular sodium overload and persistent muscle edema in Duchenne muscular dystrophy: a possible contributor of progressive muscle degeneration. J Neurol 259:2385–2392. doi:10.1007/s00415-012-6512-8

Weber T, Ducos M, Mulder E, Herrera F, Bruggemann GP, Bloch W, J W (2013) The specific role of gravitational accelerations for arterial adaptations. J Appl Physiol (1985) 114:387–393. doi:10.1152/japplphysiol.01117.2012

Zange J et al (2017) Using the Hephaistos orthotic device to study countermeasure effectiveness of neuromuscular electrical stimulation and dietary lupin protein supplementation, a randomised controlled trial. PLoS One 12:e0171562. doi:10.1371/journal.pone.0171562